

AUGMENTED REALITY BY DEPTH CAMERA FOR IMAGE-BASED PIPELINE INSPECTION

Takuma Yorimitsu, Hiroshige Dan, Akira Kobayashi and Yoshihiro Yasumuro

Faculty of Environmental and Urban Engineering, Kansai University, Japan

ABSTRACT: *This paper proposes an augmented reality (AR) investigation system that focuses on examinations of underground pipelines in situations where excavations are difficult or unnecessary. Currently, industrial endoscopes combined with video cameras are among the primary tools used in such situations, but when severe damage is found and repair work is required, above and underground conditions around the damaged section of pipe often cannot be easily verified. In our scenario, in addition to live camera images of pipe inner surfaces, we believe it would be effective to overlay various other images onto the inspector's view so that the situation between the ground surface and inner pipe can be clarified. In normal practice, industrial endoscopes are usually inserted from maintenance hatches that are installed in pipelines at set intervals. In our prototype implementation, a visual marker is placed on the maintenance hatch and an observation camera that shows the inspector's viewpoint is prepared to support the AR system. The extended length of an endoscope mounted (or self-propelled) camera, and the direction of the pipe can then be used to capture the relative location of the camera in the pipeline. From that point, mapping the collected image onto a cylindrical three-dimensional (3D) model that shows the nominal pipeline size facilitates visualization of the situation inside the pipe. In our prototype system experiments, as the camera moves forward, the live texture-mapped 3D pipe model is properly overlaid onto a realtime video image of the exterior view of the scenery. The various overlaying viewing information was also examined in a case study.*

KEYWORDS: *Augmented reality, Pipeline inspection, Industrial endoscopy, Depth camera, Posture compensation*

1. INTRODUCTION

Maintenance schemes and strategies aimed at the reinforcement and repair of the civil infrastructure are gathering considerable attention recently as numerous developed countries face problems resulting from the deterioration of decades-old infrastructures. Water pipelines, which have various uses such as potable water supply, sewerage, agricultural irrigation, and so on, are among such typical aging infrastructures. Since most such pipeline networks are buried, it is often hard to ascertain their physical conditions before deterioration-related damages become critical. However, dealing with every deteriorated infrastructure facility in every part of a country is not realistic, especially under the prevailing severe fiscal circumstances common to aging societies.

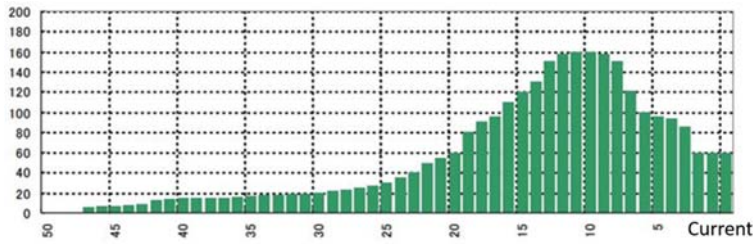


Fig. 1: (left) Newly built total pipeline length (km) vs. elapsed years (Japan Ministry of Construction and Transport, Sep. 2013). (Right) Pipeline repair work (Yoshimizu Kenki Co., Ltd. <http://www.yoshimizu.co.jp/>)

Therefore, in order to maintain the structure and functionality of existing pipelines, it is important to monitor and comprehend conditions inside and outside of the pipes *in situ*. There are two primary existing methods of inspecting such pipelines: indirect investigation from ground surface and direct investigation of pipe interiors.

Indirect investigation targets water leakage, flow volume, and corrosion by sampling the water volume, electrical potential, and soil at different points. Imaging pipe exteriors via video cameras provides another form of indirect investigation. In the case of interior investigations, the interior wall of the pipeline can be examined and diagnosed by direct measurement with a depth gauge or by visual inspections.

Direct investigations target crack conditions, snaking and/or pipeline sinking, deflection, as well as rust and sediment conditions. Thus, whereas indirect investigations provide macroscopic level information on the characteristics of existing pipelines, direct investigations are capable of ascertaining quantitative metrics of pipe configurations (Liu 2013). However, since direct investigations often require excavations to expose the pipe structures for direct access, their usage must still depend on a discrete sampling approach.

In recent years, high-resolution cameras have been installed on self-propelled, remote-controlled robots to perform examinations. Nevertheless, while color images can provide informative material for experienced operators, quantitative metrics of pipe characteristics are still required for objective investigation and management. Therefore, the purpose of this study is to propose an objective and comprehensive approach for investigating pipeline interiors that minimizes excavations.

Building information modeling (BIM) along with augmented reality (AR) techniques have recently been introduced to outdoor infrastructure maintenance workflow (Kamat, 2007, Woodward, 2010, Chi, 2013, Jiao, 2013, Park, 2013), and a number of specialized systems for underground pipeline structural maintenance have been proposed (Lawson 1998, Behzadan, 2005, Schall, 2009). One such practical service is provided in the form of Visual City by South East Corp. in Melbourne, Australia, where common information modeling (CIM) of

underground municipal gas and water pipelines has been prepared, and where onsite AR visualization is achieved on mobile devices such as tablet personal computers (PCs). Use of this service accelerates decision-making processes from inspection to repair.

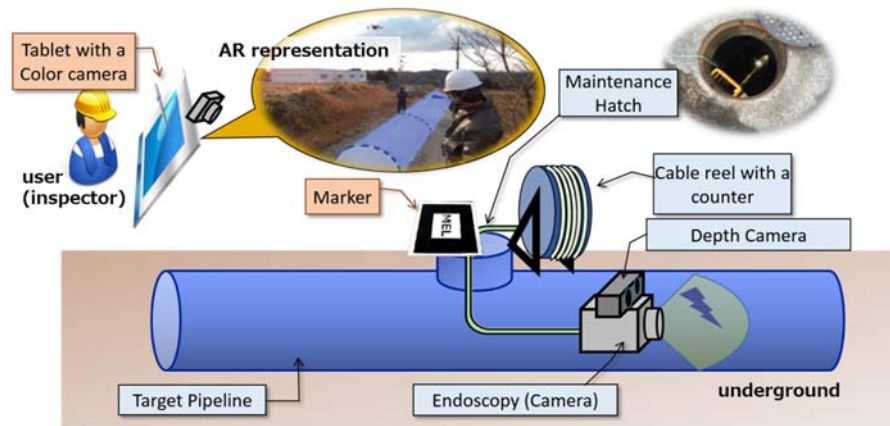


Fig. 2: Marker-based AR for realtime inspection

2. APPROACH

2.1 Marker-based AR

Existing AR applications for visualizing underground infrastructure have focused on overlaying pre-constructed underground pipeline models or computer-aided design (CAD) data onto aboveground live images. These functionalities are designed for use when planning excavations. In contrast, we have been developing an AR visualization utility for use during inspection work in order to provide more dynamic onsite assistance, as shown in Fig. 2 (Yorimitsu et al., 2015).

When using endoscopic systems, the inspector is expected to monitor and check images obtained from the camera system from a first-person perspective, which is most likely to be a distorted wide angle view, as shown in Fig. 3 (left). However, when the first-person perspective is combined with the third-person view, it provides the ability to “see” through the ground in a way that is helpful for taking the surrounding situation into account. Furthermore, a visual understanding of the relative geometry between the inspection point in the pipe structure and aboveground features and/or terrestrial conditions may potentially provide an awareness-raising environment that will assist in identifying the underlying causes of pipeline deterioration.

In our scenario, an inspection camera that can collect wide-angle color images is installed on the tip of an endoscopic cable or a self-propelled wheeled robot that can measure the camera’s travel distance and transmit that information to a host computer in realtime. We also employ another camera to capture the aboveground scenery in order to provide a “see-through” perspective from the operator’s viewpoint. A visual marker is used to provide a landmark and establish a local coordinate system at the maintenance hatch or manhole, from which the

camera system is inserted for inspection purposes.

At the start of the inspection, the initial position of the camera and the pipe direction relative to marker coordinates are recorded. Then, image-based inspection is conducted by manipulating the camera system. Based on the camera's movements, which are basically forward motion along the pipe, the camera position can be monitored by measuring the extended length of the camera cable.

Many reel-type cabled endoscopic camera systems are equipped with rotary encoding sensors that measure the length of the extended camera cable.

Our system scenario envisions a three-step process: (1) capturing live image frames from both the inspection and aboveground cameras, (2) using the inspection camera to capture raw pipe interior imagery, and (3) applying such imagery onto a texture image plane that is mapped onto the nominal size of the cylindrical model. This information is then overlaid onto the scenery image based on the relative position of the marker coordinates. Assuming that a guide device installed on the camera head basically ensures that the camera is always positioned at the center of the pipe and directed along its length, depth from the camera z and apparent radius r [pixels] on the inspection image can be expressed according to the following perspective projection:

$$z = \frac{fR - rz_0}{r},$$

where R is a physical size of the radius, z_0 is an offset depth from the camera, and f is the focal length of the camera, as shown in Fig. 3.

2.2 Camera Posture Compensation by Depth Information

Since, in practice, the camera direction always moves and often faces away from the center of the pipe during the operation, the resultant mapped texture is often distorted. In this paper, we compensate for this camera direction distortion based on normal vector distributions captured by using a depth camera combined with endoscopic camera (Inoue et al. 2015). The mesh structure of the depth image provides each normal vector n_i on each vertex i . We denote the normal vector n_i on each vertex i as follows:

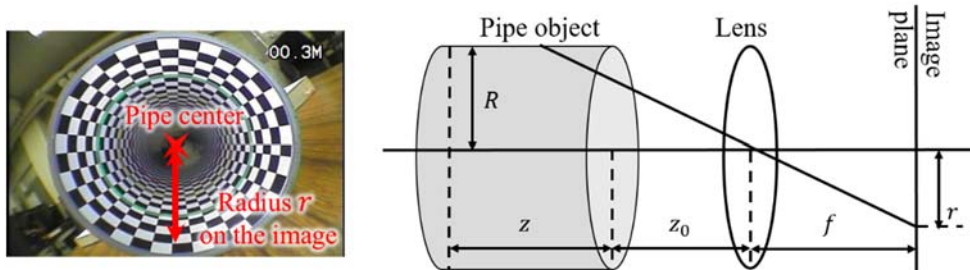


Fig. 3: AR implementation from two views: (left) marker based coordinates mapped onto a 3D model, (right) interior inspection view.

$$n_i = \begin{pmatrix} x_i \\ y_i \\ z_i \end{pmatrix} \quad (i = 1, 2, \dots, k)$$

We also define a matrix N , which is a collection of k normal vectors as

$$N = \begin{pmatrix} n_1^T \\ \vdots \\ n_k^T \end{pmatrix} \quad (k \times 3 \text{ matrix})$$

and denote the axis direction vector v along the pipe as

$$v = \begin{pmatrix} \bar{x} \\ \bar{y} \\ \bar{z} \end{pmatrix}.$$

Assuming an ideal case, vector v would be orthogonal to every normal vector n_i . In other words, each inner product Nv equals zero. Since such v does not exist due to the measurement errors and inner surface roughness, in practice, we will choose v as a solution that minimizes the squared error as follows:

$$\operatorname{argmin}_v \frac{1}{2} \|Nv\|^2 = \frac{1}{2} v^T N^T N v = \frac{1}{2} v^T M v, \quad (1)$$

where $M = N^T N$ (3×3). We simply stipulate that $\bar{z} = 1$ as a constraint in order to avoid a solution of $v = 0$. Then, equation (1) can be written as follows:

$$\operatorname{argmin}_{\bar{x}, \bar{y}} f(\bar{x}, \bar{y}) = \frac{1}{2} \begin{pmatrix} \bar{x} \\ \bar{y} \\ 1 \end{pmatrix}^T \begin{pmatrix} m_{11} & m_{12} & m_{13} \\ m_{12} & m_{22} & m_{23} \\ m_{13} & m_{23} & m_{33} \end{pmatrix} \begin{pmatrix} \bar{x} \\ \bar{y} \\ 1 \end{pmatrix} = \frac{1}{2} \begin{pmatrix} \bar{x} \\ \bar{y} \end{pmatrix}^T \begin{pmatrix} m_{11} & m_{12} \\ m_{12} & m_{22} \end{pmatrix} \begin{pmatrix} \bar{x} \\ \bar{y} \end{pmatrix} + \begin{pmatrix} m_{13} \\ m_{23} \end{pmatrix}^T \begin{pmatrix} \bar{x} \\ \bar{y} \end{pmatrix} + \frac{1}{2} m_{33} \quad (2)$$

Next, we will find (\bar{x}, \bar{y}) so that the differential of the $f(\bar{x}, \bar{y})$ equals zero.

$$Df(\bar{x}, \bar{y}) = \begin{pmatrix} m_{11} & m_{12} \\ m_{12} & m_{22} \end{pmatrix} \begin{pmatrix} \bar{x} \\ \bar{y} \end{pmatrix} + \begin{pmatrix} m_{13} \\ m_{23} \end{pmatrix} = 0$$

$$\begin{pmatrix} \bar{x} \\ \bar{y} \end{pmatrix} = - \begin{pmatrix} m_{11} & m_{12} \\ m_{12} & m_{22} \end{pmatrix}^{-1} \begin{pmatrix} m_{13} \\ m_{23} \end{pmatrix}$$

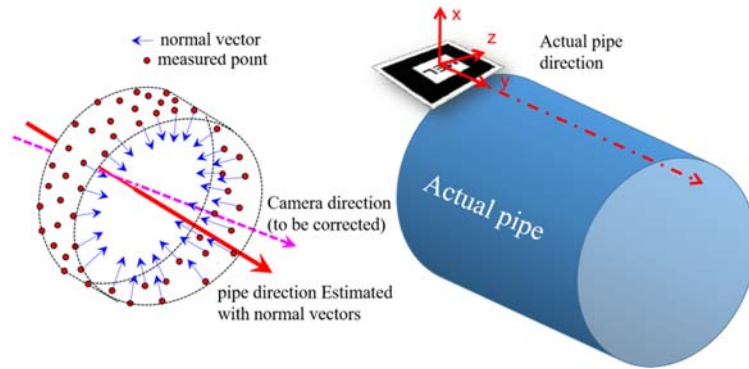


Fig. 4: AR implementation from two views: (left) marker based coordinates mapped onto a 3D model, (right) interior inspection view.

Finally, the solution of the directional vector of the pipe is $(\bar{x}, \bar{y}, 1)^T$. This direction can be aligned along the physical target pipe by finding a transformation so that the vector $(\bar{x}, \bar{y}, 1)^T$ faces parallel to one of the marker axes, according to the initial marker setup of the system, as depicted in Fig. 4.

3. EXPERIMENT

We conducted an experiment to demonstrate the proposed method using an actual endoscopic camera and a depth camera. The specifications of the inspection and depth cameras are shown in Tables 1 and 2, respectively. A 1.3 M pixel, 30 frame-per-second (FPS) universal serial bus (USB) camera (Qcam Ultra Vision, Logicool Inc.) was used to record the aboveground scenery. AR toolkit (Kato 1998) was used for implementing AR visualization software. AR toolkit provides useful application programming interfaces (APIs) for image stream capturing from multiple cameras, as well as marker-based AR handling. These include marker registration,

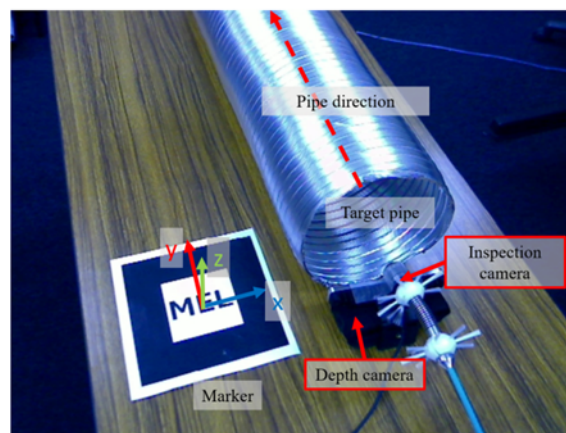


Fig. 5: Experimental setup: A marker is positioned beside the maintenance hatch, where the camera head is inserted. The head consists of jointed an endoscopy and a depth camera.

Table 1: Industrial Endoscopic Camera Specification



Field of view	160° (diagonal)	
Lens	F2.8, f = 2 mm	
Image sensor	2.5 Mpixel, 1/4" charge-coupled device (CCD)	
Frame rate	30 fps	
Distance measure	Encoding on cable drum (10 cm increments)	

Table 2: Depth Camera Specification

Device	Intel® RealSense™ SR300	
Device Size	150 × 30 × 58 mm	
Depth FoV (D × W × H)	80 × 68 × 54	
Depth FPS	30, 60	
Depth Method	Coded light IR	

camera calibration, viewing matrix estimation, and 3D object drawing in conjunction with OpenGL graphics library. We can also adjust the scaling factor that converts textured 3D objects in computer graphics along with the actual size of the pipe and camera movement distance in millimeters. The aboveground scenery camera recognizes the pre-registered visual marker and calculates the position and orientation of the inspection camera relative to the marker coordinates.

As shown in the endoscopic camera specifications, the camera cable reel is equipped with a rotary encoding sensor that is capable of counting the cable extension in 10 cm increments. Figure 5 shows the overview of our experimental setup, in which the marker is settled so that the y-axis is the direction of the target pipe. The endoscopic camera and the depth camera are fixed together and the rotational transformations between the directions of the two cameras are calculated beforehand. The pipe size is ϕ 200 mm.

Figure 6 shows an example of the depth image and the normal vector distribution captured by the depth camera, which contains 35,000 points (67,000 triangle meshes). Figure 7 shows the

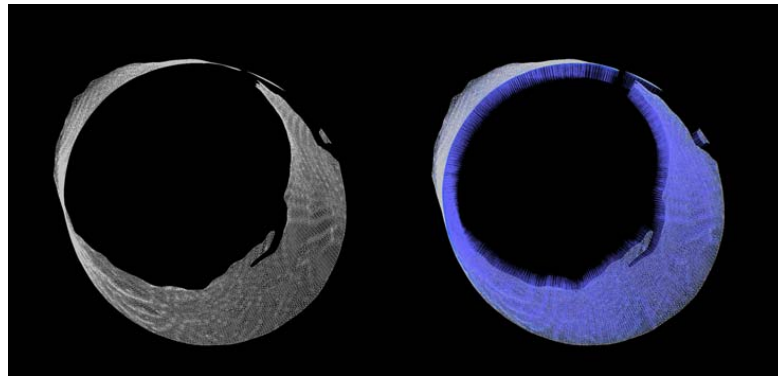


Fig. 6: (left) Captured depth data as a 3D point set, (right) the normal vectors at the points depicted by blue lines

resultant AR representation example. The left-hand side shows the original output and the right-hand side shows the result of the proposed method to compensate for the camera direction, which faces off the center of the physical pipe. Although the difference seems quite slight, the measured inner surface of the pipe is correctly aligned to the physical pipe image and the AR view is consistent with the perspective of the shooting camera. The computational cost was low enough to create an AR view in realtime.

4. CONCLUSIONS

Herein, we proposed an implementation scheme for a pipeline investigation system that combines live texturing AR representation of an actual pipeline inspection endoscopic camera with camera direction compensation functionality. Using a depth camera combined with an endoscopic camera, it was possible to overlay the inner imagery stably and correctly from the third person's perspective.

Our next step will be to validate the precision of the texture-mapped investigation images in terms of distortion and resolution, as well as the presented position on the AR representation. We are also planning actual physical inspection case studies aimed at validating the visual guidance and support functionalities of the proposed method. Our research focus will also delve deeper into the interactive AR representation design with aims toward magnifying the textured model, showing arbitrary intersections, refining imagery, creating 3D inspection histories, and so on.

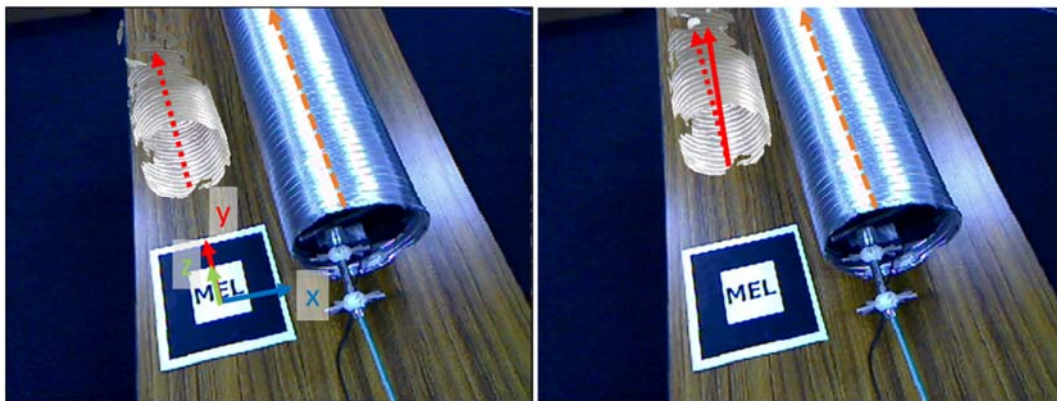


Fig. 7: Proposed method result: (left) original output, (right) output corrected via the proposed method so that the measured inner surface of the pipe model is precisely aligned with the physical target pipe.

ACKNOWLEDGMENTS

This work was partially supported by Japan Society for the Promotion of Science (JSPS) Grants-in-Aid for Scientific Research (15H02983, 16H05000).

REFERENCES

- Behzadan, A. H. and Kamat, V. R. (2005). Visualization of construction graphics in outdoor augmented reality, *Proceedings of the Winter Simulation Conference*, pp. 1914-1920.
- Chi, H. L., Kang, S. and Wang X. (2013). Research trends and opportunities of augmented reality applications in architecture, engineering, and construction, *Automation in Construction* 33, pp. 116-122.
- Hiroki Inoue, Yoshihiro Yasumuro, Hiroshige Dan, Akira Kobayashi, (2015), Deflection Computation of Pipeline Surface Based on 3D Point Cloud, Proc. of 15th International Conference on Construction Applications of Virtual Reality in Construction, Paper ID:42.
- Jiao, Y., Zhang, S., Li, Y., Wang, Y. and Yang B. (2013). Towards cloud augmented reality for construction application by BIM and SNS integration, *Automation in Construction* 33, pp. 37-47.
- Kamat, V. and El-Tawil, S. (2007). Evaluation of Augmented Reality for Rapid Assessment of Earthquake-Induced Building Damage, *Journal of Computing in Civil Engineering*, 21(5), pp. 303-310.
- Kato, H. and Billinghurst, M. (1999). Marker Tracking and HMD Calibration for a video-based Augmented Reality Conferencing System. *International Workshop on Augmented Reality (IWAR 99)*, pp. 85-94.
- Nextspace: <http://www.nextspace.co.nz/visual-city> (accessed in 2015 Jun)
- Park C., Lee D., Kwon O. and Wang X. (2013). A framework for proactive construction defect management using BIM, augmented reality and ontology-based data collection template, *Automation in Construction*, Vol. 33, pp. 61-71.
- Lawson, S. W. and Pretlove, J. R. G. (1998). Augmented reality for underground pipe inspection and maintenance. *Proc. SPIE 3524, Telemanipulator and Telepresence Technologies V*, pp. 98-104.
- Schall, G., Mendez, E., Kruijff, E., Veas, E., Junghanns, S., Reitinger, B. and Schmalstieg, D. (2009). Handheld augmented reality for underground infrastructure visualization, *Personal*

and Ubiquitous Computing, Special Issue on Mobile Spatial Interaction 13 (4) pp. 281-291.

Woodward, C., Hakkarainen, M., Korkalo, O., Kantonen, T., Aittala, M., Rainio, K. and Kähkönen, K. (2010). Mixed Reality for Mobile Construction Site Visualization and Communication, *Proceedings of 10th International Conference on Construction Applications of Virtual Reality (CONVR)*, pp. 35-44.

Takuma Yorimitsu, Hiroki Inoue, Hiroshige Dan, Yoshihiro Yasumuro, (2015) AR Presentation of Image-Based Pipeline Inspection, Proc. of 15th International Conference on Construction Applications of Virtual Reality in Construction, Paper ID:41.

Zheng L. and Kleiner Y. (2013) State of the art review of inspection technologies for condition assessment of water pipes, *Measurement* 46. 1, pp. 1-15.